Nucl Med Mol Imaging (2011) 45:139–144
DOI 10.1007/s13139-010-0071-7

CASE REPORT

# Intratumoral Heterogeneous F-18 Fluorodeoxyglucose Uptake Corresponds with Glucose Transporter-1 and Ki-67 Expression in a Case of Krukenberg Tumor: Localization of Intratumoral Hypermetabolic Focus by Fused PET/MR Image

**Hyung-Jun Im · Yong-il Kim · Woo Ho Kim · Seung Hyup Kim · Keon Wook Kang**

Received: 1 July 2010 / Accepted: 6 December 2010 / Published online: 6 January 2011


**Abstract** The expression of glucose transporters (Glut-1, Glut-3), hexokinase-II, and Ki-67 has been proposed to explain intratumoral heterogeneous F-18 fluorodeoxyglucose (FDG) uptake. We report a case of Krukenberg tumor with intratumoral heterogeneous FDG uptake which corresponded well with the expression levels of Glut-1 and ki-67. Fused positron emission tomography (PET)/magnetic resonance (MR) imaging was helpful for localizing the metabolically active area in the tumor specimen. This report elucidates the relationship between the intratumoral heterogeneous FDG uptake and biologic heterogeneity, and shows the usefulness of PET/MR in research on intratumoral heterogeneity.

**Keywords** FDG · PET/CT · PET/MRI · Glut-1 · Ki-67 · Krukenberg tumor

H.-J. Im · Y.-i. Kim · K. W. Kang
Department of Nuclear Medicine,
Seoul National University College of Medicine,
28, Yeongeon-dong, Jongno-gu,
Seoul 110-799, South Korea

W. H. Kim
Department of Pathology,
Seoul National University College of Medicine,
Seoul, South Korea

S. H. Kim
Departments of Radiology, Seoul National University Hospital,
Seoul, South Korea

K. W. Kang (✉)
Cancer Research Institute, Seoul National University,
Seoul, South Korea
e-mail: kangkw@snu.ac.kr

## Introduction

Heterogeneous intratumoral F-18 fluorodeoxyglucose (FDG) uptake is observed in some types of benign and malignant tumors [1, 2], and Kidd et al. [2] reported that intratumoral metabolic heterogeneity indicates a higher risk of lymph node involvement at diagnosis, poorer response to therapy, and a greater risk of pelvic recurrence in cervical cancer.

Some experiments have been performed to clarify the relation between heterogeneous FDG uptake and biologic heterogeneity, which is known to be related to variations in tumor responsiveness to treatment [3, 4], degree of vascularity [5], hypoxia [6–8], and tumor cellular metabolism, and intratumoral gene expression [9, 10]. Zhao et al. [11] examined the biologic mechanism responsible for a heterogeneous intratumoral FDG distribution in a rat malignant tumor model, and found that intratumoral FDG distributions corresponded well with the intratumoral expression of glucose transporter 1 (Glut-1), glucose transporter 3 (Glut-3), and hexokinase-II. Thus, they concluded that the expression levels of these proteins might contribute to the degree of FDG accumulation. In addition, Baardwijk et al. [12] reported a correlation between heterogeneous intratumoral FDG uptake and histologic patterns, such as vital tumor and fibrotic regions in human non-small cell lung cancer specimens, but immunohistochemistry was not performed.

Here, we describe a case of a Krukenberg tumor which showed heterogeneous FDG uptake by preoperative FDG positron emission tomography (PET)/computed tomography (CT), in an attempt to elucidate the biologic mechanism responsible for this phenomenon.

## Case Report

A 35-year-old woman with resectable advanced gastric cancer underwent subtotal gastrectomy in May 2006 and adjuvant chemotherapy over the following 6 months. However, in December 2009 huge bilateral pelvic masses were revealed during a routine abdominal CT follow-up. The patient was further examined by pelvic magnetic resonance (MR) imaging and a whole-body FDG PET/CT scan and for serum tumor markers, which showed increased CA 19-9 and CA 125 levels [680 U/ml (normal range <37 U/ml) and 69.7 U/ml (normal range <35 U/ml), respectively]. FDG PET/CT was performed using a PET/CT scanner (Biograph16 Hi-Res, Siemens, Germany). After fasting for at least 6 h, appropriate blood sugar level was checked (<180 mg/dl). Then the patient was injected with 9.25 MBq of FDG per kilogram of body weight, and images were acquired 1 h later. CT was performed for attenuation correction, and subsequently, emission scanning was performed from the skull base to the proximal thigh. Images were reconstructed using an iterative algorithm (ordered-subset expectation maximization). To quantify FDG uptakes, standardized uptake values (SUVs) were calculated as follows: SUV = [decay-corrected activity (kBq) per milliliter of tissue volume]/[injected FDG activity (kBq) per body mass (g)].

Pelvic MR images showed bilateral ovarian masses of heterogeneous low-signal intensity in T2-weighted images. The masses were mainly solid with multiple small intratumoral cysts, and lobulated but smooth margins. These right and left ovarian masses had maximum diameters of 12.5 cm and 5.2 cm, respectively. After injection of gadolinium-based contrast agent, the masses showed strong enhancement. (Fig. 1a-c).

In whole-body PET/CT images, the bilateral ovarian masses showed mildly increased metabolic activity with a focal markedly active portion in the anterior region of the right ovarian mass (Fig. 1d). The maximum SUV (SUVmax) of the most metabolically active portion was 6.8. On the other hand, the other part of both ovarian masses showed relatively mild FDG uptake (SUVmax 2.1). However, this metabolically active area did not show stronger gadolinium enhancement in MR image than other areas of the tumor (Fig. 1c).

The patient underwent bilateral salpingo-oophorectomy, and the pathologic diagnosis was of metastatic adenocarcinoma from gastric cancer. To investigate the biologic mechanism responsible for the heterogeneous FDG uptake, pathologic specimens were re-reviewed. No necrotic region or residual ovarian tissue was observed in the gross specimen of the right ovarian mass. To identify the precise location of the most metabolically active area in the right tumor specimen, we matched the T2-weighted coronal MR image with the gross specimen (Fig. 2a, b). We performed software-based image fusion of MR coronal images and FDG PET images (Fig. 2a, c, d), using a semi-automatic algorithm in Syngo Multi Modality Workplace (Syngo Multi Modality Workplace/Siemens Medical Systems, Erlangen, Germany). Alignment in all three planes was assessed by checking the margins of adjacent metabolically active organs (bladder, bones) and the

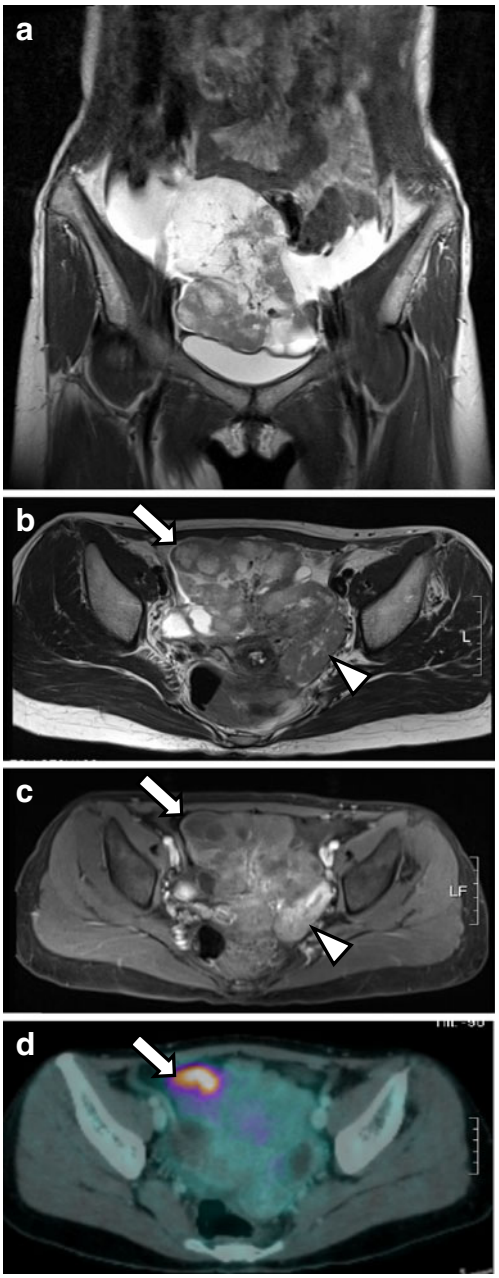


**Fig. 1** **a** T2-weighted coronal MR image showing a large right ovarian mass with a lobulated margin and heterogeneous signal intensity. **b** T2-weighted axial MR image showing a larger right ovarian mass (*arrow*) and a smaller left ovarian mass (*arrowhead*). **c** Contrast-enhanced fat-suppressed T1-weighted axial MR image showing heterogeneous enhancement of masses. **d** Axial fused FDG PET/CT image showing mild hypermetabolic tumor with the most metabolically active focus in the right anterior portion (*arrow*)

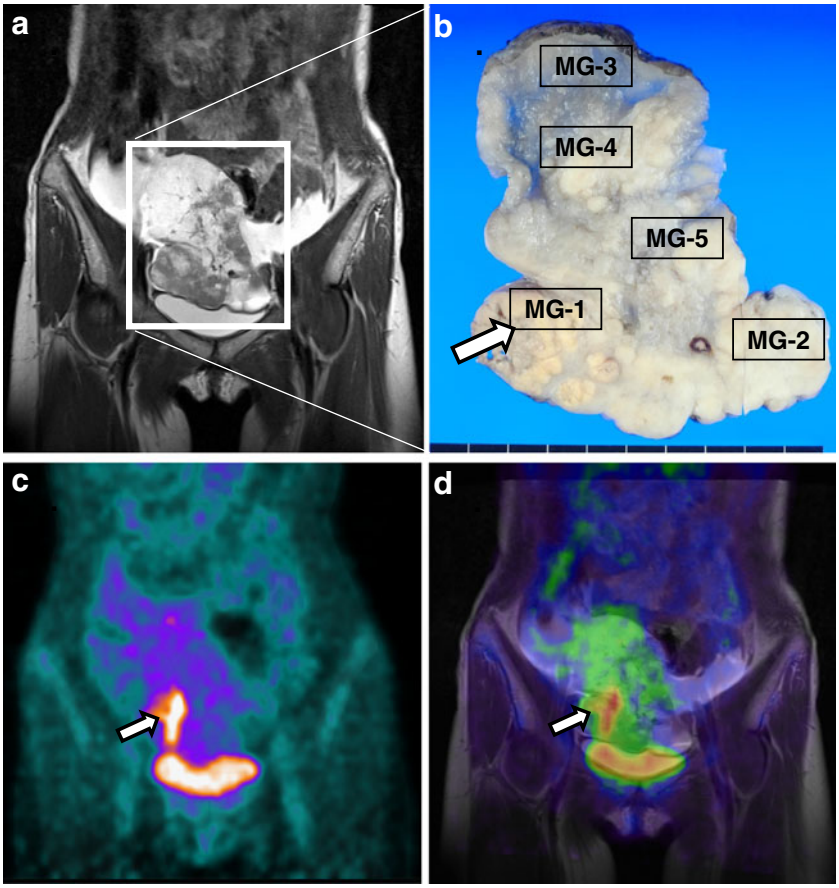


**Fig. 2** **a** T2-weighted coronal MR image showing a large right ovarian mass with a lobulated margin and heterogeneous signal intensity. **b** Photograph of the same section shown in **a** showing its heterogeneous character. Five areas (*MG1–MG5*) of this tumor, including the metabolically active region (*MG1*, *arrow*) were selected for immunohistochemical studies. **c** Coronal PET image showing mild hypermetabolism on right ovarian mass with the most hypermetabolic focus on right lower portion (*arrow*). **d** Fused PET/MR coronal image revealing the anatomical location of the hypermetabolic focus, which lies in the right lower region of the mass (*arrow*)

linearity of the hip margin. After verification, the most metabolically active area (MG1) and four other tumor regions (MG2–MG5) of the right-side tumor were selected (Fig. 2b). The SUVmax of these five regions were 6.8, 2.1, 1.7, 2.1, and 1.9, respectively.

To elucidate the biologic mechanism underlying the heterogeneous FDG uptake, we initially compared tumor cellularities in the five tumor regions. However, no significant difference was found. Immunostaining for Ki-67, Glut-1, hexokinase-II, and CD31 were performed in each tumor region sampled. Table 1 summarizes all antibodies, dilutions, antigen retrieval methods and detection methods used. The presence of Glut-1 tumor cell membrane staining and tumor cell cytoplasmic staining for hexokinase-II was expressed by percentage of tumor cells with positive staining. The intensity of staining was categorized as none (0), weak staining (1), medium staining (2), and intense staining (3). The immunoreactive level was calculated by multiplication of the scores (intensity × percent positive). For Ki-67, percentages of immunostaining positive cells were measured by counting tumor cell numbers, i.e. the number of distinctly stained nuclei per 1,000 tumor cells in the most representa-

**Table 1** Summary of immunohistochemistry methods

| Antibody | Company | Type | Dilution | Antigen retrieval | Detection |
|---|---|---|---|---|---|
| Glut-1 | Thermo Scientific | Rabbit polyclonal | 1:150 | ERS, 100°C, 20 min | BPR |
| Ki-67 | DAKO | Mouse monoclonal | 1:100 | ERS, 100°C, 20 min | BPR |
| Hexokinase-II | Santa-cruz | Goat polyclonal | 1:100 | Citr, MW | ABC |
| CD31 | DAKO | Mouse monoclonal | 1:50 | Citr, MW | ABC |

*Thermo Scientific* Thermo Fisher Scientific; *DAKO* Dako Patts, Glostrup, Denmark; *Santa-cruz* Santa Cruz Biotechnology, Santa Cruz, California; *ERS* Epitope Retrieval solution 1, pH 6.0; *Citr* citrate buffer, pH 6.0; *MW* microwave 750 W for 15 min; *BPR* Bond Polymer Refine Detection Kit (Leica Microsystems, Bannockburn, Ill.); *ABC* Elite vector avidin-biotin enzyme complex kit (Vector Laboratories)

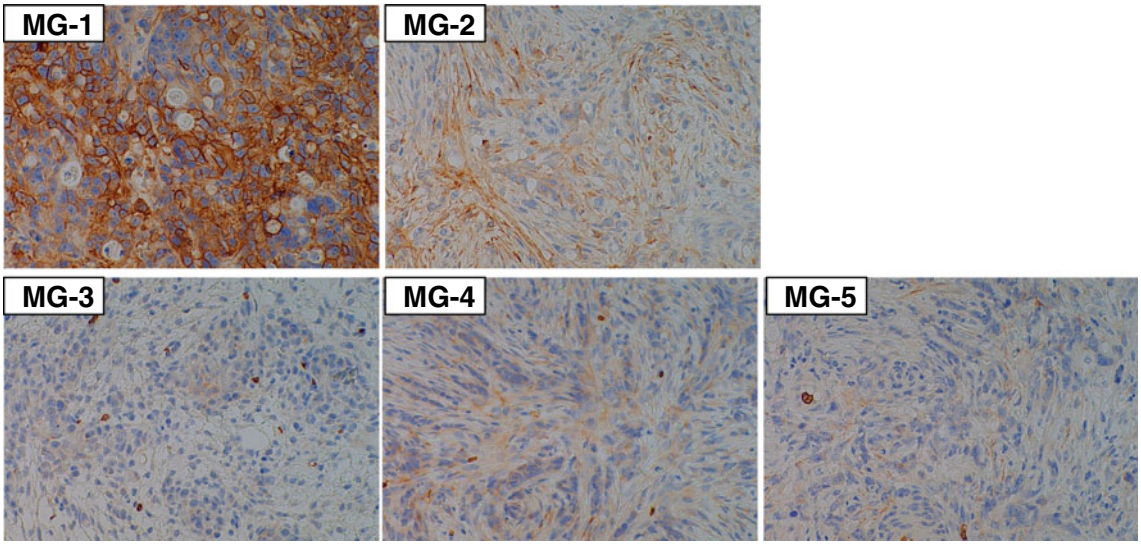


**Fig. 3** Glut-1 immunohistochemical staining of the five tumor areas (*MG1–MG5*) showing markedly increased cytoplasmic and membranous expressions of Glut-1 in the MG1 than in the other areas (original magnification, 200×)

tive area at a magnification of 400×. Microvessel density (MVD) was assessed based on the method by Bossi et al. [13]. Immunoreactive levels of Glut-1 in the five tumor regions (MG1–MG5) were 255, 25, 14, 20, and 12, respectively. The labeling indexes of Ki-67 expression in the five tumor regions (MG1–MG5) were 38.9%, 16.1%, 12.1%, 14.3%, and 9.5%, respectively. The immunoreactive level of Glut-1 and the labeling index of Ki-67 were found to be markedly elevated in the most metabolically active region (MG1) (Figs. 3, 4). On the other hand, the immunoreactive level of hexokinase-II and MVD of MG1 were not the highest among the five regions. The immunoreactive levels of hexokinase-II in the five tumor regions (MG1-MG5) were 90, 48, 50, 104, and 44, respectively. The MVDs of the five tumor regions (MG1–MG5) were 27, 40, 32, 15, and 12, respectively. Lastly, correlation analysis between expression level of those markers and SUVmax in the five tumor regions were performed. Immunoreactive level of Glut-1 and labeling index of Ki-67 of the five tumor regions showed significant correlation with SUVmax ($r^2$=0.99, $P$<0.0001; $r^2$=0.97, $P$=0.002) (Fig. 5a, b). On the contrary, the immunoreactive level of hexokinase-II and MVD of the five tumor regions showed no significant correlation with SUVmax ($P$=n.s., $P$=n.s.) (Fig. 5c, d). Statistical analysis

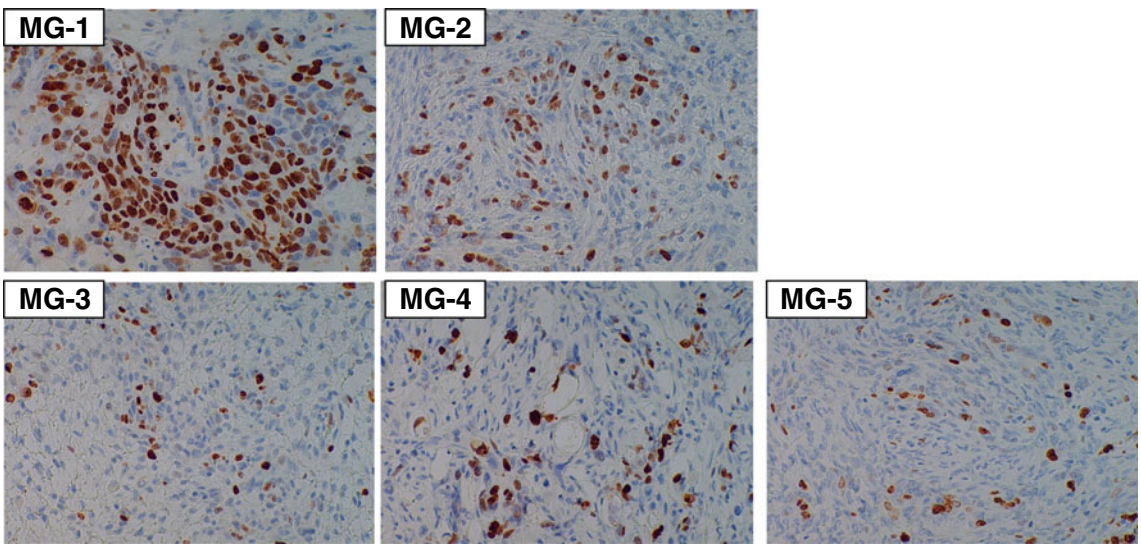


**Fig. 4** Ki-67 immunohistochemical staining of the five tumor areas (*MG1–MG5*) showing markedly increased expressions of Ki-67 in MG1 than in the other areas (original magnification, 200×)

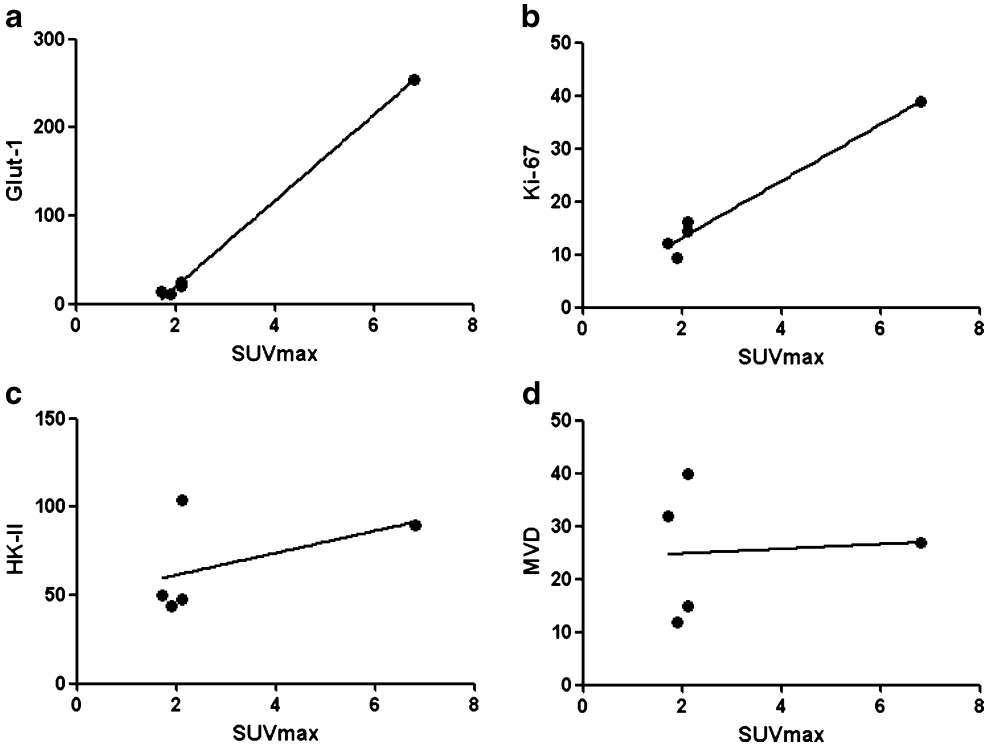


**Fig. 5** Correlation between SUVmax and immunoreactive level of Glut-1 ($r^2$=0.99, $P$< 0.0001, **a**), labeling index of Ki-67 ($r^2$=0.97, $P$=0.002, **b**), immunoreactive level of hexokinase-II ($P$ = n.s., **c**), and MVD ($P$ = n.s., **d**). *HK-II* hexokinase-II

was done by MedCalc (MedCalc Software). $P$ values of less than 0.05 were considered significant.

## Discussion

Focal high intratumoral FDG uptake can be caused by either a nonmalignant component in the tumor or heterogeneity of a malignant component within the tumor. For a nonmalignant component, the area of intratumoral necrosis is the most common cause of focal high intratumoral FDG uptake. The reason for high FDG accumulation in necrotic regions is mainly due to macrophage aggregation, caused by active inflammation [14]. Other causes of nonmalignant high intratumoral FDG uptake include a residual ovary which may contain functional cysts or corpus luteum in patients with primary or metastatic ovarian tumors [15].

Heterogeneity within the malignant component of the tumor—for example, heterogeneous intratumoral cell proliferation, or regional hypoxia—can also cause heterogeneous intratumoral FDG uptake [16]. Immunostaining has often been used to investigate these phenomena—for example, Ki-67 is known to reflect tumor proliferation [17, 18], HIF-1α is known to be related to hypoxic conditions [19], and Glut-1, Glut-3, and hexokinase-II are known to be related to increased glucose utilization [11, 19].

Accordingly, many studies have shown that SUVmax values are correlated with the expression of Glut-1, Glut-3, hexokinase, and Ki-67 in malignant tumors [17, 19]. However, the heterogeneous intratumoral expression of these proteins, causing focal high SUVmax, have not been previously reported in human cases. In the present study, we demonstrate that intratumoral heterogeneous FDG uptake corresponds with the level of expression of Ki-67 and Glut-1 through image-pathology correlation. However, whether the immunostaining sites correspond exactly to the areas showing the intratumoral heterogeneity in FDG uptake may be a possible limitation.

We also immunostained for CD31, the expression of which is known to be correlated with microvessel density, which in turn, reflects tumor angiogenesis. However, no significant correlation was observed between MVD and SUVmax. This is consistent with the findings of a previous study, which found no positive correlation between FDG uptake and microvessel density [20].

As shown by this report, Glut-1 and Ki-67 expression levels may vary widely even in a single tumor with heterogeneous FDG uptake. Several studies have reported a correlation between SUVmax and protein expression in tumors of different patients [17, 19]. However, in these studies, no mention was made of the locations of these proteins expressed in one tumor.

Finally, we performed PET/MR image fusion to locate the hypermetabolic focus precisely on tumor specimens. MR imaging is superior to CT with respect to tumor delineation and soft tissue contrast [21, 22], and thus, MR

imaging is more feasible than CT in terms of matching with tumor specimens and radiologic images. Thus, a fused PET/MR image was more beneficial than a fused PET/CT image in locating a focal hypermetabolic area in the tumor specimen in our case.

## Conclusion

Intratumoral heterogeneous FDG uptake was found to correspond well with Glut-1 and ki-67 expression in a Krukenberg tumor. Furthermore, our findings show that Glut-1 and Ki-67 levels may vary widely even in a single tumor that shows heterogeneous FDG uptake. In addition, PET/MR fusion imaging enabled us to localize a metabolically active area on a tumor specimen.

**Acknowledgements** This work was supported by the Priority Research Centers Program through the National Research Foundation of South Korea (NRF) funded by the Ministry of Education, Science and Technology (2009-0093820).

## References

1. Basu S, Nair N, Banavali S. Uptake characteristics of fluorodeoxyglucose (FDG) in deep fibromatosis and abdominal desmoids: potential clinical role of FDG-PET in the management. Br J Radiol. 2007;80:750–6.
2. Kidd EA, Grigsby PW. Intratumoral metabolic heterogeneity of cervical cancer. Clin Cancer Res. 2008;14:5236–41.
3. Britten RA, Evans AJ, Allalunis-Turner MJ, Franko AJ, Pearcey RG. Intratumoral heterogeneity as a confounding factor in clonogenic assays for tumour radioresponsiveness. Radiother Oncol. 1996;39:145–53.
4. Hockel M, Schlenger K, Aral B, Mitze M, Schaffer U, Vaupel P. Association between tumor hypoxia and malignant progression in advanced cancer of the uterine cervix. Cancer Res. 1996;56:4509–15.
5. Delorme S, Knopp MV. Non-invasive vascular imaging: assessing tumour vascularity. Eur Radiol. 1998;8:517–27.
6. Pugachev A, Ruan S, Carlin S, Larson SM, Campa J, Ling CC, et al. Dependence of FDG uptake on tumor microenvironment. Int J Radiat Oncol Biol Phys. 2005;62:545–53.
7. Thomlinson RH, Gray LH. The histological structure of some human lung cancers and the possible implications for radiotherapy. Br J Cancer. 1955;9:539–49.
8. Thorwarth D, Eschmann SM, Paulsen F, Alber M. A model of reoxygenation dynamics of head-and-neck tumors based on serial 18 F-fluoromisonidazole positron emission tomography investigations. Int J Radiat Oncol Biol Phys. 2007;68:515–21.
9. Bachtiary B, Boutros PC, Pintilie M, Shi W, Bastianutto C, Li JH, et al. Gene expression profiling in cervical cancer: an exploration of intratumor heterogeneity. Clin Cancer Res. 2006;12:5632–40.
10. Lee AW. Nasopharyngeal cancer: advances in radiotherapy. Int J Radiat Oncol Biol Phys. 2007;69:S115–7.
11. Zhao S, Kuge Y, Mochizuki T, Takahashi T, Nakada K, Sato M, et al. Biologic correlates of intratumoral heterogeneity in 18 F-FDG distribution with regional expression of glucose transporters and hexokinase-II in experimental tumor. J Nucl Med. 2005;46:675–82.
12. van Baardwijk A, Bosmans G, van Suylen RJ, van Kroonenburgh M, Hochstenbag M, Geskes G, et al. Correlation of intra-tumour heterogeneity on 18 F-FDG PET with pathologic features in non-small cell lung cancer: a feasibility study. Radiother Oncol. 2008;87:55–8.
13. Bossi P, Viale G, Lee AK, Alfano R, Coggi G, Bosari S. Angiogenesis in colorectal tumors: microvessel quantitation in adenomas and carcinomas with clinicopathological correlations. Cancer Res. 1996;55:5049–53.
14. Kubota R, Yamada S, Kubota K, Ishiwata K, Tamahashi N, Ido T. Intratumoral distribution of fluorine-18-fluorodeoxyglucose in vivo: high accumulation in macrophages and granulation tissues studied by microautoradiography. J Nucl Med. 1992;33:1972–80.
15. Ames J, Blodgett T, Meltzer C. 18 F-FDG uptake in an ovary containing a hemorrhagic corpus luteal cyst: false-positive PET/CT in a patient with cervical carcinoma. AJR Am J Roentgenol. 2005;185:1057–9.
16. Kubota R, Kubota K, Yamada S, Tada M, Ido T, Tamahashi N. Active and passive mechanisms of [fluorine-18] fluorodeoxyglucose uptake by proliferating and prenecrotic cancer cells in vivo: a microautoradiographic study. J Nucl Med. 1994;35:1067–75.
17. Nguyen XC, Lee WW, Chung JH, Park SY, Sung SW, Kim YK, et al. FDG uptake, glucose transporter type 1, and Ki-67 expressions in non-small-cell lung cancer: correlations and prognostic values. Eur J Radiol. 2007;62:214–9.
18. Hommura F, Dosaka-Akita H, Mishina T, Nishi M, Kojima T, Hiroumi H, et al. Prognostic significance of p27KIP1 protein and ki-67 growth fraction in non-small cell lung cancers. Clin Cancer Res. 2000;6:4073–81.
19. van Baardwijk A, Dooms C, van Suylen RJ, Verbeken E, Hochstenbag M, Dehing-Oberije C, et al. The maximum uptake of (18)F-deoxyglucose on positron emission tomography scan correlates with survival, hypoxia inducible factor-1alpha and GLUT-1 in non-small cell lung cancer. Eur J Cancer. 2007;43:1392–8.
20. Guo J, Higashi K, Ueda Y, Oguchi M, Takegami T, Toga H, et al. Microvessel density: correlation with 18 F-FDG uptake and prognostic impact in lung adenocarcinomas. J Nucl Med. 2006;47:419–25.
21. Chung NN, Ting LL, Hsu WC, Lui LT, Wang PM. Impact of magnetic resonance imaging versus CT on nasopharyngeal carcinoma: primary tumor target delineation for radiotherapy. Head Neck. 2004;26:241–6.
22. von Schulthess GK, Schlemmer HP. A look ahead: PET/MR versus PET/CT. Eur J Nucl Med Mol Imaging. 2009;36(Suppl 1):S3–9.